

ESTIMATION OF GEOPHYSICAL LOADINGS OVER THE MALAYSIAN
REGION BASED ON KINEMATIC PRECISE POINT POSITIONING GPS
TECHNIQUE

NUR SURAYATUL ATIKAH BINTI ALIHAN

A thesis submitted in fulfilment of the
requirements for the award of the degree of
Master of Philosophy

Faculty of Built Environment and Surveying
Universiti Teknologi Malaysia

NOVEMBER 2018

DEDICATION

*Special dedicated to
my dearly loved family*

ACKNOWLEDGEMENT

بِسْمِ اللَّهِ الرَّحْمَنِ الرَّحِيمِ

In the name of Allah, the most Merciful and Beneficent

Alhamdulillah, first and foremost, I give all praise to Almighty Allah for giving me strength, knowledge, ability and opportunity to undertake this research study.

In my journey towards this master's degree, I have found teachers, an inspiration, a role model and a pillar of support in my career, Dr. techn. Dudy Darmawan Wijaya and Dr. Ami Hassan bin Md. Din. They have always been there providing their heartfelt support, invaluable guidance, encouragement, motivation and suggestions in my quest for knowledge. I am eternally being grateful to them for their assistance and supervision because this thesis would not have been possible without their guidance.

I would like to express my gratitude to team members of Geomatic Innovation Research Group (GnG) UTM, Assoc. Prof. Kamaludin, Mr. Rusli and Assoc. Prof. Dr. Tajul Ariffin Musa, for their support and knowledge sharing throughout my study. My sincere appreciations to all my comrades who have provided assistance and moral support at various occasions specially Noor Nabilah, Astina, Nur Fadila, Nornajihah, Amalina, Dr. Nazirah, Noor Anim Zanariah, Dr. Wan Anom, Khalilah, Adilla, Hanif, Nizam and Dr. Yusuf Opaluwa. Their views and tips are useful indeed. I also extend my acknowledgement for those who have not been mentioned here.

Shall not be forgotten, I also deeply appreciate to Geodesy Research Group (KKGD) family for all the supports and cooperation, especially during my attachment of the internship program. Thank you Prof. Ir. Hasanuddin Zainal Abidin and Dr. Ir. Kosasih Prijatna for allowing me to undertake the internship program within the Department of Geodesy and Geomatic Engineering, Faculty of Earth Sciences and

Technology, Institute of Technology Bandung, not forgetting the care, friendship, knowledge and understanding enjoyed from them including Dr. Ir. Bambang Setyadji, Dr. Irwan Gumilar, Dr. Heri Andreas, Dr. Ir. Dina Anggreni Sarsito, Dr. Ir. Vera Sadarviana, Ir. Mipi, Pak Teguh, Dr. techn. Dhota Pradipta, Brian Bramanto, Jessy Kartini, Fajar Trihantoro, Irsyad Kharisma and the host of others for giving me home away from home in KKGD and made my stay in Indonesia memorable. I would like to extend my utmost appreciation and gratitude to Ibu Nerytha Khotimah for her heartfelt support, encouragement, motivation and inspiration in my life.

Finally, my deep and sincere gratitude to the biggest source of my strength, my beloved family. The blessing and unconditional love from my father and mother, Alihan bin Ibrahim and Rohayah binti Ali, and the love and care of my brother, Muhammad Hafizuddin and sisters, Nur Atirah and Nur Atifah, who stands by my side and spiritually supporting me during the course of my study. I am forever indebted to my parents for giving me the opportunities and experiences that have made me who I am. They selflessly encouraged me to explore new directions in life and seek my own destiny. This journey would not have been possible if not for them, and I dedicated this milestone to them. Thank you so much for believing and always be there for me.

ABSTRACT

The earth's crust undergoes natural deformation due to the geophysical loadings that consist of the earth body tide, ocean tide loading, atmospheric pressure loading and pole tide. This periodic displacement is generated by the changes of the gravitational attraction between the moon and the sun acting upon the earth's rotation, along with the temporal atmospheric changes and the variability of the ocean tide. The study of the geophysical loadings is important in the geodesy field as the magnitude of the signals is significant and can contribute to errors in space geodetic measurements such as Global Positioning System (GPS), Very-Long Baseline Interferometry (VLBI) and Altimeter. This study aims to estimate the spatio-temporal variation of the geophysical loadings due to the earth body tide, ocean tide loading and the total signals of the earth tide over the Malaysian region, based on the GPS observations by using a Kinematic Precise Point Positioning (KPPP) GPS approach. Continuous GPS observations over a one-year period in the year 2013 have been utilised to observe the diurnal, semi-diurnal and long-term periods of tidal constituents. The tidal analysis of harmonic and spectral are conducted to examine the characteristic of the geophysical loadings as well as to estimate the tidal parameters of the tidal constituents. The results of the geophysical loadings derived from the KPPP GPS solutions correlate well with the predictions of the theoretical models, IERS2003 and NAO.99b, with the correlation coefficient above 0.90 at three components: north, east and up. The root mean square error (RMSE) is less than ± 1 cm at north and east components and around ± 6 cm at up component for both earth body tide and earth tide. The RMSE is minimal at all components of ocean tide loading. The presence of the geophysical loadings indicates that as many as 76% to 93% of the geophysical loadings signal are contained in the GPS time series. The findings reveal that earth body tide signals are more significant if compared to ocean tide loading signals because the magnitude of the earth body tide is greater than that of the ocean tide loading and it affects the coordinate system particularly at up component. The spatio-temporal variation of the geophysical loadings is generated during the apogee and perigee phenomena, monsoon seasons and throughout the year 2013 to provide the information on the temporal changes from the geophysical loadings response. Results have widened the understanding of geophysical loadings variations in equatorial regions and illustrated the potential of GPS to provide the local parameters of the geophysical loadings that are beneficial for earth tidal modelling and that can be used to improve the quality of space geodetic measurements.

ABSTRAK

Permukaan kerak bumi mengalami deformasi semula jadi disebabkan oleh beban geofizik yang terdiri daripada pasang surut kerak bumi, beban pasang surut air laut, beban tekanan atmosfera dan pasang surut kutub. Anjakan berkala ini terhasil daripada perubahan tarikan graviti antara bulan dan matahari yang bertindak ke atas putaran bumi di samping perubahan atmosfera dan perubahan pasang surut air laut. Kajian mengenai beban geofizik adalah penting dalam bidang geodesi kerana magnitud isyarat yang dinyatakan adalah ketara dan boleh menyumbang kepada kesalahan pengukuran geodetik angkasa seperti Sistem Penentuan Global (GPS), Interferometri Asas Sangat Panjang (VLBI) dan Altimeter. Kajian ini adalah untuk menganggarkan variasi ruang-masa beban geofizik akibat daripada pasang surut kerak bumi, beban pasang surut air laut dan jumlah isyarat pasang surut bumi di rantau Malaysia berdasarkan pemerhatian GPS dengan menggunakan pendekatan ketepatan titik penentuan kinematik jitu (KPPP) GPS. Cerapan GPS yang berterusan sepanjang tempoh setahun pada tahun 2013 digunakan untuk memerhatikan jujuk pasang surut diurnal, separuh diurnal dan jujuk jangka panjang. Analisis pasang surut harmonik dan spektral dijalankan untuk mengkaji ciri-ciri beban geofizik dan juga untuk menganggarkan parameter jujuk pasang surut. Hasil beban geofizik yang diperolehi daripada KPPP GPS berkorelasi baik dengan ramalan model teori, IERS2003 dan NAO.99b, dengan pekali korelasi di atas 0.90 bagi komponen utara, timur dan ketinggian. Minimum selisih punca kuasa dua (RMSE) adalah kurang daripada ± 1 cm bagi komponen utara dan timur dan dalam anggaran ± 6 cm bagi komponen ketinggian untuk pasang surut kerak bumi dan pasang surut bumi. RMSE adalah minimum di semua komponen beban pasang surut air laut. Kewujudan beban geofizik menunjukkan bahawa sebanyak 76% hingga 93% isyarat beban geofizik terkandung dalam siri masa GPS. Hasil kajian menunjukkan bahawa isyarat pasang surut kerak bumi adalah lebih ketara berbanding dengan beban pasang surut air laut kerana magnitud pasang surut kerak bumi lebih besar daripada beban pasang surut air laut dan ia memberi kesan kepada sistem koordinat terutamanya di komponen ketinggian. Variasi ruang-masa beban geofizik dihasilkan semasa fenomena apogee dan perigee, musim tengkujuh dan sepanjang tahun 2013 untuk memberikan maklumat tentang perubahan masa dari tindak balas beban geofizik. Keputusan dapat meluaskan pemahaman mengenai variasi beban geofizik di kawasan khatulistiwa dan ia menunjukkan potensi GPS dalam menyediakan parameter beban geofizik tempatan yang bermanfaat untuk pemodelan pasang surut bumi dan dapat digunakan untuk meningkatkan kualiti pengukuran geodetik.

TABLE OF CONTENTS

	TITLE	PAGE
	DECLARATION	i
	DEDICATION	ii
	ACKNOWLEDGEMENT	iii
	ABSTRACT	v
	ABSTRAK	vi
	TABLE OF CONTENTS	vii
	LIST OF TABLES	xi
	LIST OF FIGURES	xiii
	LIST OF ABBREVIATIONS	xviii
	LIST OF SYMBOLS	xx
	LIST OF APPENDICES	xxiii
CHAPTER 1	INTRODUCTION	1
1.1	Background of the Study	1
1.2	Statement of the Problem	4
1.3	Research Objectives	6
1.4	Scope of the Study	7
1.5	Significance of the Study	8
1.6	Research Framework	9
	1.6.1 Phase 1: Literature Review and Planning	10
	1.6.2 Phase 2: The Correspondence of the Geophysical Loadings with the Theoretical Models	11
	1.6.3 Phase 3: The Tidal Analysis	11
	1.6.4 Phase 4: The Visualisation of the Geophysical Loadings Response over the Malaysian Region	12
1.7	Structure of the Thesis	12
CHAPTER 2	LITERATURE REVIEW	15
2.1	Introduction	15

2.2	Tides	15
2.2.1	Tides Generating Potential	16
2.2.2	Tidal Analysis	19
2.2.3	The Prediction of Tides	22
2.2.4	Tidal Spectral Analysis	22
2.2.5	The Mechanism of Semi-diurnal, Diurnal and Long-term Tidal Constituents	24
2.3	Geophysical Loadings	25
2.3.1	Earth Body Tide	26
2.3.2	Ocean Tide Loading	28
2.3.3	Atmospheric Pressure Loading	28
2.3.4	Pole Tide	29
2.4	The Sensors for Geophysical Loadings Determination	30
2.4.1	GPS in Geophysical Loadings Study	31
2.4.2	GPS CORS Networks in Malaysia	32
2.5	The Prior Studies of the Geophysical Loadings Estimation	33
2.6	Concluding Remarks	41
CHAPTER 3	RESEARCH METHODOLOGY	43
3.1	Introduction	43
3.2	GPS Observations and Processing Methods	43
3.2.1	Estimation of Earth Body Tide, Ocean Tide Loading and Earth Tide based on KPPP GPS Observations	45
3.2.2	Data Cleaning and Filling the Data Gap	47
3.3	The Applicability of the Predictions from Theoretical Models	50
3.4	The Computation of the Correlation between the Geophysical Loadings based on KPPP GPS Solutions with the Predictions of Theoretical Models	51
3.5	Evaluate the Presence of Earth Body Tide, Ocean Tide Loading and Earth Tide Signals in GPS Observations using General Least Squares Approaches	53
3.6	Tidal Analysis	57
3.7	Concluding Remarks	58

CHAPTER 4	THE CORRELATION OF THE GEOPHYSICAL LOADINGS BASED ON KPPP GPS OBSERVATIONS WITH THE PREDICTIONS OF THEORETICAL MODELS	59
4.1	Introduction	59
4.2	The Correlation between the Geophysical Loadings based on KPPP GPS Solutions with the Predictions of Theoretical Models	59
4.2.1	Earth Body Tide	59
4.2.2	Ocean Tide Loading	74
4.2.3	Earth Tide	88
4.3	The Presence of Earth Body Tide, Ocean Tide Loading and Earth Tide Signals in GPS Observations	102
4.4	Concluding Remarks	106
CHAPTER 5	THE CHARACTERISTIC OF EARTH BODY TIDE, OCEAN TIDE LOADING AND EARTH TIDE OBSERVED BY KPPP GPS	107
5.1	Introduction	107
5.2	Tidal Harmonic Analysis	107
5.2.1	Tidal Harmonic Analysis of Earth Body Tide	109
5.2.2	Tidal Harmonic Analysis of Ocean Tide Loading	120
5.2.3	Tidal Harmonic Analysis of Earth Tide	132
5.3	Tidal Spectral Analysis	143
5.3.1	Tidal Spectral Analysis of Earth Body Tide	143
5.3.2	Tidal Spectral Analysis of Ocean Tide Loading	149
5.3.3	Tidal Spectral Analysis of Earth Tide	155
5.4	The Spatio-temporal Variation of Earth Body Tide, Ocean Tide Loading and Earth Tide over Malaysian Region	160
5.4.1	The Spatio-temporal Variations of Earth Body Tide, Ocean Tide Loading and Earth Tide Response along the Year of 2013	160
5.4.2	The Spatio-temporal Variations of Earth Body Tide, Ocean Tide Loading and Earth Tide Response during the Apogee and Perigee Phenomenon	166

5.4.3	The Spatio-temporal Variations of Earth Body Tide, Ocean Tide Loading and Earth Tide Response during the Monsoon Seasons	168
5.5	Concluding Remarks	174
CHAPTER 6	CONCLUSION AND RECOMMENDATIONS	175
6.1	Conclusion	175
6.2	Recommendations	177
REFERENCES		179
APPENDIX A - F		187 - 388
LIST OF PUBLICATIONS		389

LIST OF TABLES

TABLE NO.	TITLE	PAGE
Table 2.1	Summary of the related studies regarding the geophysical loadings estimation.	38
Table 3.1	The processing strategies.	45
Table 3.2	The strength of correlation based on the linear correlation coefficient (Jackson, 2009).	52
Table 4.1	The statistical parameters of earth body tide at the north component.	68
Table 4.2	The statistical parameters of earth body tide at the east component.	70
Table 4.3	The statistical parameters of earth body tide at the up component.	72
Table 4.4	The statistical parameters of ocean tide loading at the north component.	82
Table 4.5	The statistical parameters of ocean tide loading at the east component.	84
Table 4.6	The statistical parameters of ocean tide loading at the up component.	86
Table 4.7	The statistical parameters of earth tide at the north component.	96
Table 4.8	The statistical parameters of earth tide at the east component.	98
Table 4.9	The statistical parameters of earth tide at the up component.	100
Table 4.10	The percentage of presence of earth body tide (EBT), ocean tide loading (OTL), earth tide (ET) and other signals (OT) in GPS observations.	104
Table 5.1	The details of tidal harmonic constituents.	108
Table 5.2	The details of amplitudes of tidal constituents of earth body tide at PEKN station.	112
Table 5.3	The details of phases of tidal constituents of earth body tide at PEKN station.	113
Table 5.4	The details of amplitudes of tidal constituents of earth body tide at SEMP station.	117

Table 5.5	The details of phases of tidal constituents of earth body tide at SEMP station.	118
Table 5.6	The summary of mean amplitude differences and mean phase differences of the tidal constituents of earth body tide.	119
Table 5.7	The details of amplitudes of tidal constituents of ocean tide loading at PEKN station.	123
Table 5.8	The details of phases of tidal constituents of ocean tide loading at PEKN station.	124
Table 5.9	The details of amplitudes of tidal constituents of ocean tide loading at SEMP station.	129
Table 5.10	The details of phases of tidal constituents of ocean tide loading at SEMP station.	130
Table 5.11	The summary of mean amplitude differences and mean phase differences of the tidal constituents of ocean tide loading.	131
Table 5.12	The details of amplitudes of tidal constituents of earth tide at PEKN station.	135
Table 5.13	The details of phases of tidal constituents of earth tide at PEKN station.	136
Table 5.14	The details of amplitudes of tidal constituents of earth tide at SEMP station.	140
Table 5.15	The details of phases of tidal constituents of earth tide at SEMP station.	141
Table 5.16	The summary of mean amplitude differences and mean phase differences of the tidal constituents of earth tide.	142
Table 5.17	The summary of the earth body tide, ocean tide loading and earth tide displacement during apogee and perigee phenomenon.	167
Table 5.18	The summarize of the earth body tide, ocean tide loading and earth tide displacement during the monsoon seasons.	173

LIST OF FIGURES

FIGURE NO.	TITLE	PAGE
Figure 1.1	The geophysical setting of Malaysia (Hall <i>et al.</i> , 2008).	1
Figure 1.2	The forces that affect the earth rotation and the coordinate system (Dickey, 1995).	2
Figure 1.3	The initial of the receiver position is displaced from $(\chi R^0, \gamma R^0, ZR^0)$ to $(\chi R', \gamma R', ZR')$ due to the geophysical loadings effect.	5
Figure 1.4	The distribution of MyRTKnet stations around Malaysia.	7
Figure 1.5	The research framework of the study.	9
Figure 2.1	Newton's law of gravitation.	16
Figure 2.2	The tide generating force between the moon and the earth.	17
Figure 2.3	The semi-diurnal tidal cycle occurrence twice a day. The unit of the tidal height is in meter (Berg, 2017).	25
Figure 2.4	The diurnal tidal cycle occupying once a day. The unit of the tidal height is in meter (Berg, 2017).	25
Figure 2.5	The distribution of MyRTKnet stations in Peninsular Malaysia (DSMM, 2012).	32
Figure 2.6	The distribution of MyRTKnet stations in Sabah and Sarawak (DSMM, 2012).	33
Figure 2.7	(a) the raw superconducting gravimeter data (δg_{raw}) and (b) the theoretical earth body tide model, Wahr-Dehant model (Neumeyer, 2010).	34
Figure 2.8	The network stations of VLBI around the world (Schuh and Behrend, 2012; Behrend, 2017).	35
Figure 2.9	The example of the time series from the one month of observations, May 2006. (a) – (c) The KPPP GPS time series (red) with the time series from the combination of the theoretical earth tidal model (green) at the three components of displacement. (d) The KPPP GPS time series (red) with the time series of superconducting gravimeter (green) (Ito <i>et al.</i> , 2009).	37
Figure 3.1	Main work flow of GPS data processing using RTKLIB.	44
Figure 3.2	The GPS time series with the outliers (○) and data gap (□).	48

Figure 3.3	The GPS time series after removing the outliers.	49
Figure 3.4	The GPS time series after filling the data gap using the harmonic method of tidal prediction.	49
Figure 3.5	The comparison of IERS2003 model (green) with the earth body tide observations from the superconducting gravimeter (blue) (Pahlevi <i>et al.</i> , 2017).	50
Figure 3.6	The relationship between two variables based on the value of linear correlation coefficient (Roberts, 2017).	52
Figure 3.7	The fitting points between two configurations.	56
Figure 4.1	The time series of earth body tide variation at the BIN1 station for the period of January 1, 2013 to December 31, 2013. Blue and red lines are the earth body tide observations and the earth body tide model, respectively.	60
Figure 4.2	The time series of earth body tide variation at the BIN1 station for the period of January 1, 2013 to February 28, 2013. Blue and red lines are the earth body tide observations and the earth body tide model, respectively.	61
Figure 4.3	The strong positive correlation of earth body tide observations based on KPPP GPS solutions and IERS2003 model of BIN1 station.	62
Figure 4.4	The time series of earth body tide variation at the MERS station for the period of January 1, 2013 to February 28, 2013. Blue and red lines are the earth body tide observations and the earth body tide model, respectively.	63
Figure 4.5	The relationship of earth body tide observations based on KPPP GPS solutions and IERS2003 model at MERS station.	64
Figure 4.6	The time series of earth body tide variation at the CAME station for the period of January 1, 2013 to February 28, 2013. Blue and red lines are the earth body tide observations and the earth body tide model, respectively.	65
Figure 4.7	The relationship of earth body tide observations based on KPPP GPS solutions and IERS2003 model at CAME station.	66
Figure 4.8	The low frequency trend of ocean tide loading at BIN1 station for the period of January 1, 2013 to December 31, 2013. Blue and red colours represent the ocean tide loading observations based on KPPP GPS and ocean tide loading model, respectively.	74
Figure 4.9	The time series of ocean tide loading at BIN1 station for the period of January 1, 2013 to February 28, 2013. Blue and red	

	lines are the ocean tide loading derived from the KPPP GPS and the theoretical ocean tide loading model, respectively.	75
Figure 4.10	The relationship of ocean tide loading derived from KPPP GPS and NAO.99b model at BIN1 stations.	76
Figure 4.11	The time series of ocean tide loading at MERS station for the period of January 1, 2013 to February 28, 2013. Blue and red lines are the ocean tide loading derived from the KPPP GPS and the theoretical ocean tide loading model, respectively.	77
Figure 4.12	The relationship of ocean tide loading derived from KPPP GPS and NAO.99b model at MERS stations.	78
Figure 4.13	The time series of ocean tide loading at CAME station for the period of January 1, 2013 to February 28, 2013. Blue and red lines are the ocean tide loading derived from the KPPP GPS and the theoretical ocean tide loading model, respectively.	79
Figure 4.14	The relationship of ocean tide loading derived from KPPP GPS and NAO.99b model at CAME stations.	80
Figure 4.15	The time series of earth tide variation at the BIN1 station for the period of January 1, 2013 to December 31, 2013. Blue and red lines are the earth tide observations based on KPPP GPS solutions and the earth tide model, respectively.	88
Figure 4.16	The time series of earth tide variation at BIN1 station for the period of January 1, 2013 to February 28, 2013. Blue and red lines are the earth tide derived from the KPPP GPS and earth tide from the theoretical models, respectively.	89
Figure 4.17	The relationship of earth tide derived from KPPP GPS and earth tide from the theoretical models at BIN1 stations.	90
Figure 4.18	The time series of earth tide variation at MERS station for the period of January 1, 2013 to February 28, 2013. Blue and red lines are the earth tide derived from the KPPP GPS and earth tide from the theoretical models, respectively.	91
Figure 4.19	The relationship of earth tide derived from KPPP GPS and earth tide from the theoretical models at MERS stations.	92
Figure 4.20	The time series of earth tide variation at CAME station for the period of January 1, 2013 to February 28, 2013. Blue and red lines are the earth tide derived from the KPPP GPS and earth tide from the theoretical models, respectively.	93
Figure 4.21	The relationship of earth tide derived from KPPP GPS and earth tide from the theoretical models at CAME stations.	94
Figure 4.22	The average of presence signals in GPS observations.	103

Figure 5.1	The amplitudes of tidal constituents of earth body tide at PEKN stations.	110
Figure 5.2	The phases of tidal constituents of earth body tide at PEKN stations.	111
Figure 5.3	The amplitudes of tidal constituents of earth body tide at SEMP stations.	115
Figure 5.4	The phases of tidal constituents of earth body tide at SEMP stations.	116
Figure 5.5	The amplitudes of tidal constituents of ocean tide loading at PEKN station.	121
Figure 5.6	The phases of tidal constituents of ocean tide loading at PEKN station.	122
Figure 5.7	The amplitudes of tidal constituents of ocean tide loading at SEMP station.	127
Figure 5.8	The phases of tidal constituents of ocean tide loading at SEMP station.	128
Figure 5.9	The amplitudes of tidal constituents of earth tide at PEKN station.	133
Figure 5.10	The phases of tidal constituents of earth tide at PEKN station.	134
Figure 5.11	The amplitudes of tidal constituents of earth tide at SEMP station.	138
Figure 5.12	The phases of tidal constituents of earth tide at SEMP station.	139
Figure 5.13	The general view of tidal spectral analysis of earth body tide at PEKN station.	145
Figure 5.14	The power spectral density of earth body tide time series at PEKN station.	146
Figure 5.15	The general view of tidal spectral analysis of earth body tide at SEMP station.	147
Figure 5.16	The power spectral density of earth body tide time series at SEMP station.	148
Figure 5.17	The general view of tidal spectral analysis of ocean tide loading at PEKN station.	151
Figure 5.18	The power spectral density of ocean tide loading time series at PEKN station.	152

Figure 5.19	The general view of tidal spectral analysis of ocean tide loading at SEMP station.	153
Figure 5.20	The power spectral density of ocean tide loading time series at SEMP station.	154
Figure 5.21	The general view of tidal spectral analysis of earth tide at PEKN station.	156
Figure 5.22	The power spectral density of earth tide time series at PEKN station.	157
Figure 5.23	The general view of tidal spectral analysis of earth tide at SEMP station.	158
Figure 5.24	The power spectral density of earth tide time series at SEMP station.	159
Figure 5.25	The average propagation of the earth body tide displacement at time 00:00:00 hour to 03:00:00 hour during 2013. X-axis is longitude and Y-axis is latitude.	163
Figure 5.26	The average propagation of the ocean tide loading displacement at time 00:00:00 hour to 03:00:00 hour during 2013. X-axis is longitude and Y-axis is latitude.	164
Figure 5.27	The average propagation of the earth tide displacement at time 00:00:00 hour to 03:00:00 hour during 2013. X-axis is longitude and Y-axis is latitude.	165
Figure 5.28	The average of earth body tide displacement during monsoon seasons.	170
Figure 5.29	The average of ocean tide loading displacement during monsoon seasons.	171
Figure 5.30	The average of earth tide displacement during monsoon seasons.	172

LIST OF ABBREVIATIONS

3D	- three-dimensional
ATX	- antenna phase variation center
CLK	- IGS final clock
CORS	- Continuously Operating Reference System
CPD	- cycle per day
CUI	- Comment User Interface
DCB	- Differential Code Bias
DORIS	- Doppler Orbitography and Radiopositioning Integrated by Satellite
DSMM	- Department of Survey and Mapping Malaysia
ERP	- Earth Rotation Parameter
FFT	- Fast Fourier Transform
GIS	- Geographic Information System
GMT	- Generic Mapping Tools
GNSS	- Global Navigation Satellite System
GOTIC2	- Global Oceanic Tidal Correction
GPS	- Global Positioning System
IGS	- International GPS/GNSS Service
IHO	- International Hydrographic Organization
K1	- luni-solar diurnal
K2	- luni-solar semi-diurnal
KPPP	- Kinematic Precise Point Positioning
M2	- principal lunar semi-diurnal
Mf	- lunar fortnightly
Mm	- lunar monthly
MyRTKnet	- Malaysian Real-Time Kinematic GNSS Network
N2	- larger lunar elliptic semi-diurnal

- O1 - principal lunar diurnal
- P1 - principal solar diurnal
- Q1 - larger lunar elliptic diurnal
- RMSE - root mean square error
- RTKLIB - Real-Time Kinematic Library
- S2 - principal solar semi-diurnal
- SP3 - precise ephemeris
- Ssa - solar semi annual
- VLBI - Very Long Baseline Interferometry

LIST OF SYMBOLS

F_a	-	the attraction force of particle A
F_b	-	the attraction force of particle B
F	-	the attraction force between both particle A and B
G	-	the gravitational constant ($6.674 \times 10^{-11} \text{ N m}^2 \text{ kg}^{-2}$)
M_a	-	mass of particle A
M_b	-	mass of particle B
c	-	the distance between the center of the mass of both particle A and B
E	-	center of the earth
M	-	center of the moon
Q	-	the point on the earth's surface
F_Q	-	the attraction force of particle at point Q
M_m	-	mass of the moon ($7.35 \times 10^{22} \text{ kg}$)
b	-	the distance of the particle at point Q to the center of the moon
a	-	the distance of particle at point Q from the center of the earth
θ	-	the angle at the center of the earth between EM and EQ
A_o	-	the coefficient
n	-	the tidal constituents
A_n	-	amplitude of the tidal constituent n
ω_n	-	angular frequency of the tidal constituent n
t	-	time epoch
θ_n	-	the phase of the tidal constituent n
a_n	-	coefficients of series
b_n	-	coefficients of series
X	-	unknown parameter
L	-	observation data
A	-	design matrix
E_{Total}	-	total energy
f_s	-	sampling frequencies

f_h	-	highest frequencies
$f(\eta)$	-	frequency in cycles per unit time
Δt	-	sampling interval
Z	-	the length of data
j	-	the j^{th} tidal data
E_s	-	Energy Spectral Density
n, m	-	degree and order
h_{mn}	-	Love numbers
l_{mn}	-	Shida numbers
$\Delta \vec{r}$	-	the vector displacement of the station
GM_e	-	the gravitational parameter of the earth
GM_j	-	the gravitational parameter of the moon ($j=2$) or the sun ($j=3$)
\hat{R}_j, R_j	-	the unit vector from the geocenter of the earth to the moon or sun, and it's magnitude
R_e	-	equatorial radius of the earth ($R_e = 6\,378\,136.6\text{ m}$)
\hat{r}, r	-	the unit vector from the geocenter of the earth to station, and it's magnitude
h_2	-	the nominal degree 2 Love number ($h_2 = 0.6078$)
l_2	-	the nominal degree 2 Shida number ($l_2 = 0.0847$)
Δc_k	-	the tidal displacement of component k
Δr	-	vertical displacement
p	-	local air pressure anomaly
\bar{p}	-	average of the pressure anomaly
$\Delta \lambda$	-	displacement longitudinal
$\Delta \theta$	-	displacement latitudinal
\widehat{EBT}	-	earth body tide derived from KPPP GPS
\widehat{OTL}	-	ocean tide loading derived from KPPP GPS
\widehat{ET}	-	earth tide derived from KPPP GPS
\overline{EBT}	-	earth body tide model, IERS2003
\overline{OTL}	-	ocean tide loading model, FES2012
$\mathcal{E}_{\overline{EBT}}$	-	earth body tide model error
$\mathcal{E}_{\overline{OTL}}$	-	ocean tide loading model error

UCL	-	upper control limit
CL	-	control limit
LCL	-	lower control limit
χ	-	mean
σ	-	standard deviation
R	-	linear correlation coefficient
h	-	number of pairs data
x	-	the predictions of the theoretical model data
y	-	the observations of geophysical loadings based on KPPP GPS solutions
v_x	-	residuals of data x
v_y	-	residuals of data y
m	-	gradient of the straight line
V_e	-	residual vector
l'_i	-	the second iterations of observations
l_i	-	original observations
v_i	-	residuals of the observations
P_{EBT}	-	presence of the earth body tide
P_{OTL}	-	presence of ocean tide loading
P_{ET}	-	presence of earth tide

LIST OF APPENDICES

APPENDIX	TITLE	PAGE
Appendix A	Tidal Harmonic Parameters of Earth Body Tide	187
Appendix B	Tidal Harmonic Parameters of Ocean Tide Loading	231
Appendix C	Tidal Harmonic Parameters of Earth Tide	275
Appendix D	Spatio-temporal Variations of Earth Body Tide, Ocean Tide Loading and Earth Tide Response along the Year of 2013	319
Appendix E	Spatio-temporal Variations of Earth Body Tide, Ocean Tide Loading and Earth Tide Response during Apogee and Perigee Phenomenon	349
Appendix F	Spatio-temporal Variations of Earth Body Tide, Ocean Tide Loading and Earth Tide Response during Monsoon Seasons	385

CHAPTER 1

INTRODUCTION

1.1 Background of the Study

Malaysia, geographically located in the Sunda Plate, is surrounded by the South China Sea, the Andaman Sea and the Straits of Malacca towards the north and the south of Peninsular Malaysia, respectively, while the Sulu Sea along with the Celebes Sea and the Makassar Strait are located near Sabah and Sarawak as shown in Figure 1.1. This country is exposed to various types of natural hazards such as land subsidence, landslides, earthquakes and natural deformation phenomena as it close to the one of the most active seismic plate boundaries between the Indo-Australian and Eurasian Plate (Yong, 2013). This exposure indicates the implication toward the coordinate system, geodetic positioning, and deformation study in Malaysia.

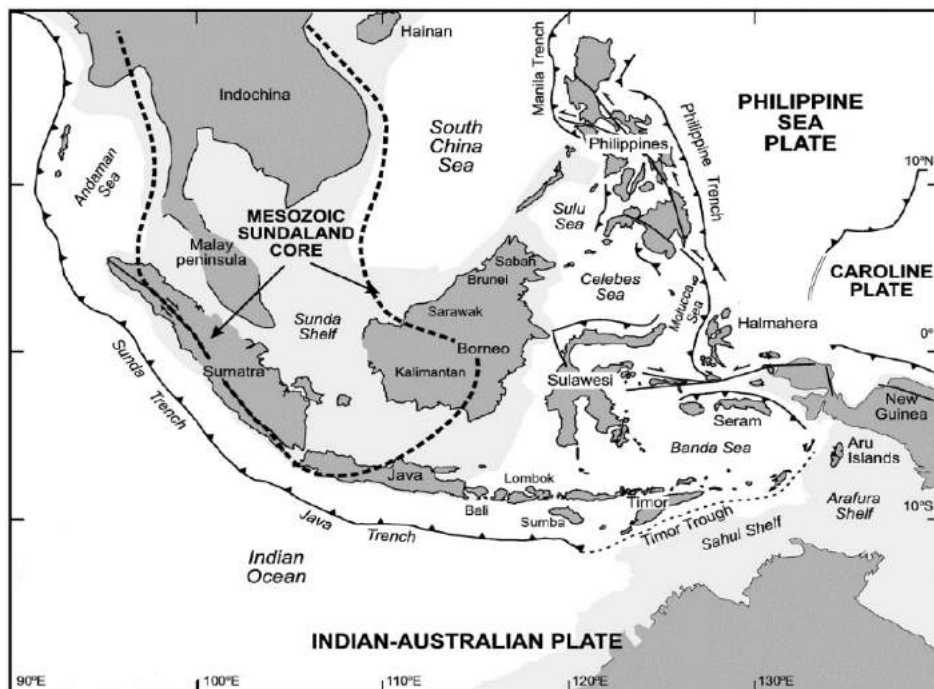


Figure 1.1 The geophysical setting of Malaysia (Hall *et al.*, 2008).

Generally, the realization of the reference coordinate system used in the satellite geodesy demands a good understanding about the dynamic of the earth. As eloquently stated by Abidin (2001), the dynamic of the earth has a wide spectrum from the scale of the galaxy to the scale of the local movement underneath the earth's crust. There are three types of earth dynamic that affect the coordinate system in satellite geodesy, which are the earth orbit around the sun alongside with the other planets, the earth rotation about its axis and the relatively slow movement of the earth's crust. The rotation of the earth has been affected by the gravitational force between the moon and the sun, the geophysical movement of mass distribution within the solid earth, ocean tide loading, atmospheric loading, and plate tectonic motions (Dickey, 1995; Abidin, 2001). Figure 1.2 illustrates the forces that perturb the rotation of the earth and the coordinate system.

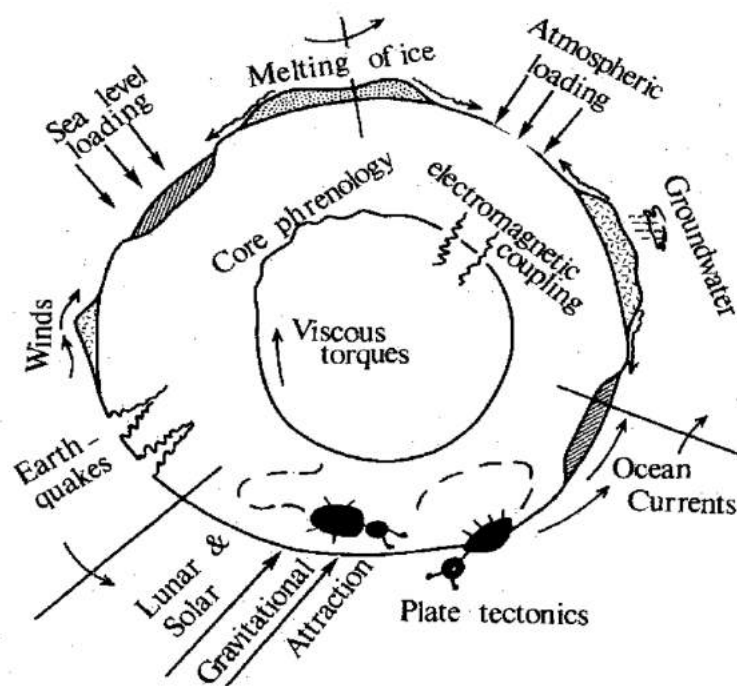


Figure 1.2 The forces that affect the earth rotation and the coordinate system (Dickey, 1995).

Recently, with the high demand for precise measurement, the knowledge of the dynamic of the earth has become important in the field of geodesy. Thus, this study widened the understanding of the dynamic of the earth due to the geophysical loadings phenomena in the Malaysian region. The periodic ground displacements due to the changes of gravitational attraction between the moon and the sun along with the

varying of the ocean tide referred as earth body tide and ocean tide loading, respectively (Agnew, 2009; Bos *et al.*, 2015). The earth body tide is the largest periodic motion of the earth's crust compared to ocean tide loading which it can reach in the centimeter (cm) level of displacements, about 5 cm in the horizontal plane and 20-30 cm in the vertical component (H eroux and Kouba, 2001; Zheng, 2007; Cai, 2009). However, the loading effect of the ocean tide loading can be large as the geodetic stations are very close to the shore (Pagiatakis, 1988). As explained by Agnew (2009), there are three important parts of the tidal deformations in geophysics. First, the facts about the earth will be obtained from the measurement of the tidal deformations. Second, the tidal effects against the geodetic measurement can be eliminated by using the models of the tidal deformations. Third, these models can be used to investigate the impact of the tidal variations towards the geophysical phenomenon such as earthquakes, tsunami and volcanic activity (Agnew, 2009).

Conventionally, the precise point measurement of tidal response is commonly measured by various instruments such as super-conducting gravimeters, strain meter and tilt observations. However, the rising cost of operation, the less data provided, the sparse distribution of station and the difficulty of accessing the best location for low-noise site causes inconsistent observations to expose the spatial heterogeneity of the solid earth tidal field (Ito *et al.*, 2009). With the advent of precise space geodetic techniques such as Very Long Baseline Interferometry (VLBI) and Global Positioning System (GPS), it is possible to determine geophysical characteristics of tidal deformations *i.e.* earth tide (the sum of earth body tide and ocean tide loading), ocean tide loading, and earth body tide (Vey *et al.*, 2002; Ito *et al.*, 2009; Bos *et al.*, 2015). Furthermore, the studies that used the technology of GPS have achieved millimeter-level accuracy in tidal measurements which have better precision than superconducting gravimeter (Yuan *et al.*, 2013).

Since the VLBI stations are limited worldwide, the study utilised the operational GPS Continuously Operating Reference System (CORS) existing in Malaysia which is the Malaysian Real-Time Kinematic GNSS Network (MyRTKnet) operated by the Department of Survey and Mapping Malaysia (DSMM). These GPS CORS networks currently are widely used to support various applications such as

precise positioning, surveying, navigation, mapping and research studies. Furthermore, the GPS CORS does not drift during strong ground motion, provide an absolute measurement and is cheaper in terms of installation and maintenance. These advantages lead to the study of using GPS to investigate the spatio-temporality of earth tidal deformations in the Malaysian region.

1.2 Statement of the Problem

Malaysia's crust undergoes periodic displacements due to the gravitational attraction between the moon and the sun, temporally varying atmospheric, surface loads, oceanic and continental water mass. The gravitational force and ocean tide water movement periodically load and unload the earth causing the changes of displacement, tilt and gravity. The most significant changes are directly underneath the load such as on the sea floor (Pagiatakis, 1988). This periodic ground displacement affects the coordinate system and has gained importance in geodesy as the high precision of space geodetic measurements (*e.g.* GPS, VLBI, Doppler Orbitography and Radiopositioning Integrated by Satellite (DORIS) and Altimeter) required the correction from the tidal effects to maximize their extensive use in geodesy and geophysical studies such as monitoring the variations of mean sea level and quantifying the vertical land motion (Agnew, 2009). Thus, to increase the accuracy of satellite positioning and geodetic measurement techniques to sub-millimeter level, a good knowledge of the tidal deformation is imperative.

Equation (1.1) represented the example of the mathematical model for GPS positioning (El-Rabbany, 2002; Hofmann-Wellenhof *et al.*, 2007).

$$L_{L2} = \rho + c(dt^s - dt_R) - dion_{L2} + dtrop + (dH^s + dH_R)_{L2} + dmp_{L2} + \lambda_{L2}N_{L2} + E_{L2} \quad (1.1)$$

where L_{L2} is the carrier phase measurement on L2 frequency, ρ is pseudorange, $dion$ is ionospheric delay, $dtrop$ is tropospheric delay, dH^s and dH_R are satellite and receiver hardware, respectively, dmp is the multipath effect and E is the measurement noise.

From the equation (1.1), there are parameter known as pseudorange that estimated from satellite position (χ^s, γ^s, Z^s) and initial receiver position $(\chi_{R^0}, \gamma_{R^0}, Z_{R^0})$ that can be expressed as follows (El-Rabbany, 2002; Hofmann-Wellenhof *et al.*, 2007):

$$\rho_{R^0}^s = \sqrt{(\chi^s(t) - \chi_{R^0}(t))^2 + (\gamma^s(t) - \gamma_{R^0}(t))^2 + (Z^s(t) - Z_{R^0}(t))^2} \quad (1.2)$$

If the GPS observation in the static mode, it can be assumed that the initial of the receiver position is remain unchanged. However, due to the existing of the geophysical loadings, the initial of receiver position are actually displaced to $(\chi_{R'}, \gamma_{R'}, Z_{R'})$ as shown in Figure 1.3.

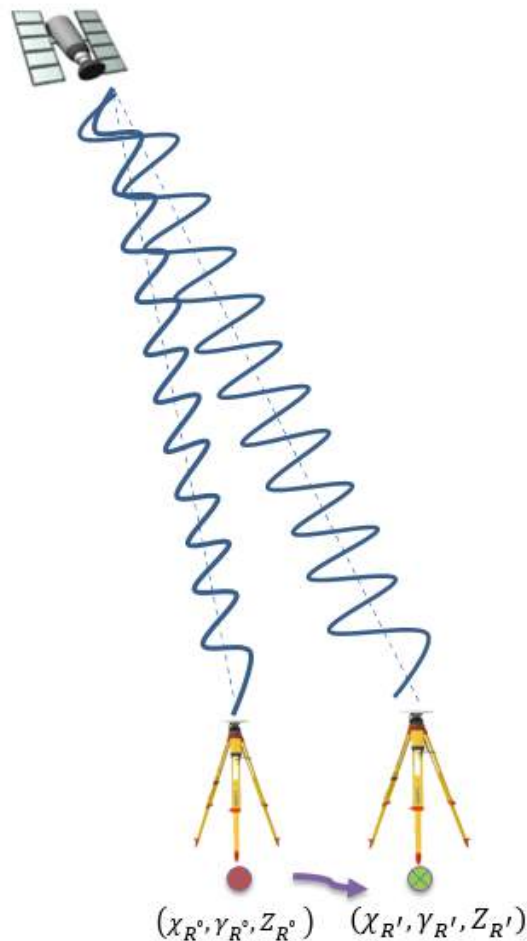


Figure 1.3 The initial of the receiver position is displaced from $(\chi_{R^0}, \gamma_{R^0}, Z_{R^0})$ to $(\chi_{R'}, \gamma_{R'}, Z_{R'})$ due to the geophysical loadings effect.

Therefore, the site displacement should be corrected by using equation (1.3) to (1.5) where $(\Delta X, \Delta Y, \Delta Z)$ is estimated from the tidal effects of the geophysical loadings.

$$\chi_{R'} = \chi_{R^0}(t) + \Delta X \quad (1.3)$$

$$\gamma_{R'} = \gamma_{R^0}(t) + \Delta Y \quad (1.4)$$

$$Z_{R'} = Z_{R^0}(t) + \Delta Z \quad (1.5)$$

With the advent of precise space geodetic techniques such as GPS and VLBI, the study of the interior of the earth from the surface observations of the loading effects can provide the consistency of observations in revealing the spatial heterogeneity of the solid earth tidal field. In this study, the technology of GPS is utilised to investigate the characteristic of the tidal displacement as Malaysia has 78 GPS CORS stations distributed between 30 to 120 km apart since the VLBI stations are limited in number, with only 35 stations available worldwide. Furthermore, several studies have utilised the GPS since around 2000 to validate the tidal displacement based on GPS with the predictions from both earth body tide models and ocean tide loading model (Ito *et al.*, 2009; Penna *et al.*, 2015).

1.3 Research Objectives

The aim of this study is to estimate the spatio-temporal variation of geophysical loadings over the Malaysian region based on GPS observations. This study has undertaken to pursue three objectives as follows:

- i. To estimate the correlation between the GPS solutions and the predictions from the theoretical earth tidal model.
- ii. To determine the tidal parameters of the earth body tide, ocean tide loading and earth tide.
- iii. To examine the characteristics of geophysical loading over the Malaysian region.

1.4 Scope of the Study

The scopes of this study are described as follows:

1. This study utilised the Malaysian Real-Time Kinematic GNSS Network (MyRTKnet) operated by the Department of Survey and Mapping Malaysia (DSMM). MyRTKnet consists of 50 and 28 GPS Continuously Operating Reference Station (CORS) over Peninsular Malaysia and East Malaysia, respectively. However, only 70 GPS observation stations with intervals of 30 seconds can be used in this study due to the other eight (8) stations having bad observations in 2013. The distribution of the MyRTKnet stations is shown in Figure 1.4.

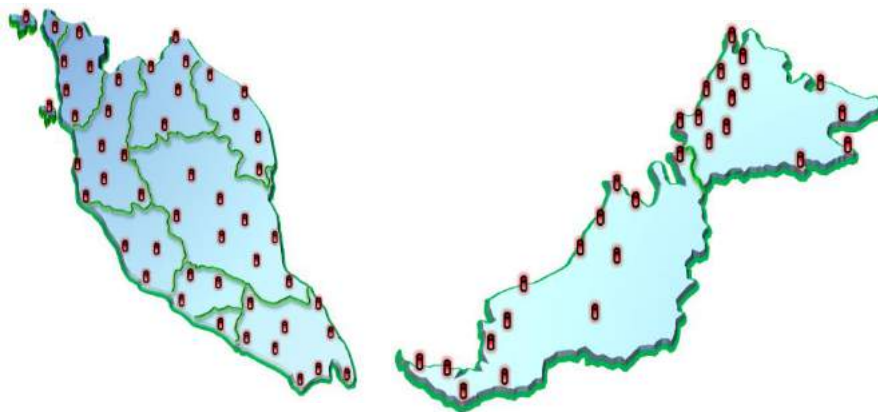


Figure 1.4 The distribution of MyRTKnet stations around Malaysia.

2. An open source software RTKLIB with Comment User Interface (CUI) is employed to process the GPS data from MyRTKnet stations using Kinematic Precise Point Positioning (KPPP) solutions.
3. This study estimates the geophysical loadings of the earth body tide, ocean tide loading and earth tide based on GPS observations. The tidal displacements observed by GPS are validated with the predictions from the theoretical model which are IERS2003 and NAO.99b for earth body tide model and ocean tide loading model, respectively.

4. The tidal spectral analysis using Fast Fourier Transform (FFT) method is performed to determine the characteristic of geophysical loadings in GPS observations. A total of 11 tidal constituents from the diurnal, semi-diurnal and long-term periods is observed. The tidal parameters, amplitude and phase of each tidal constituents are estimated using the tidal harmonic analysis method.
5. The hourly snapshots of earth tidal displacements are generated by using the Generic Mapping Tools (GMT) version 5.3.1 to investigate the spatial and temporal variations of geophysical loadings response in the Malaysia region during the perigee and apogee phenomenon, monsoon seasons and throughout the year 2013.

1.5 Significance of the Study

This study is essential for several purposes:

1. This study widened the understanding of earth tidal variations in equatorial regions. It is beneficial for earth tide modelling that include both earth body tide and ocean tide loading for improving the quality of space geodetic measurements.
2. This study provides the local tidal parameters of earth body tide, ocean tide loading and earth tide from the GPS observations that can be used in further research such as to investigate the impact of the geophysical loadings against the geohazards monitoring, to quantify the actual vertical land motion in the local region and to study the dynamics of the solid earth.
3. This study could be used to support authorities, institutions and researchers in various aspects such as providing the information of geophysical loadings over Malaysian region.

1.6 Research Framework

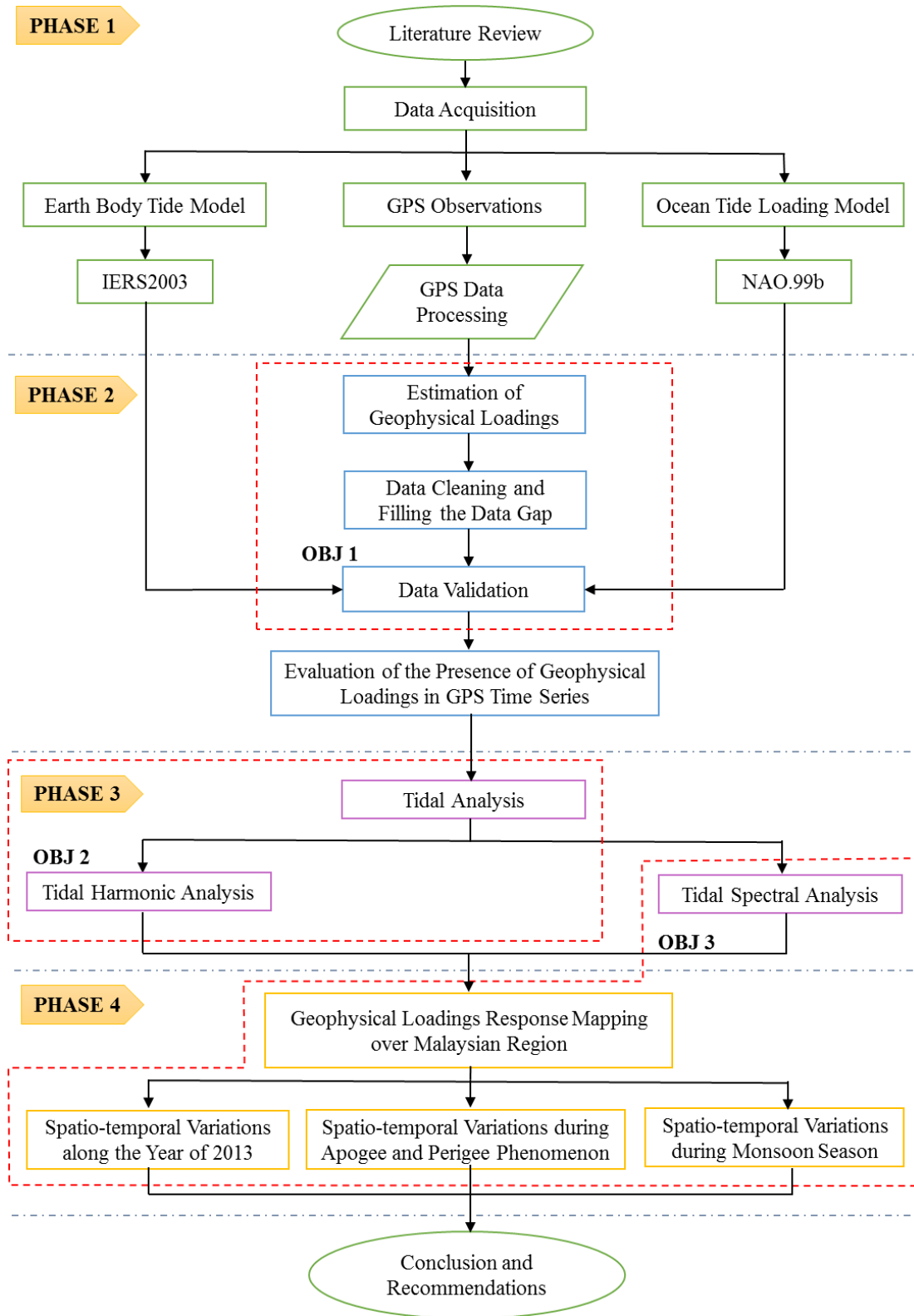


Figure 1.5 The research framework of the study.

The research methodology of this study is conducted in four phases. Phase 1 of the study is focused on the literature review of related issues such as the theory of tides, tidal analysis, the geophysical loadings and the existing sensor in Malaysia along with the data acquisition and data processing used in this study. Next, phase 2 is concerned with the estimation of the geophysical loadings from the GPS solutions and the post-data processing, which consists of the data cleaning and filling the data gap. The data validation is conducted to verify the outcome of the geophysical loadings from the GPS with the theoretical models used in this study. In addition, the presence of the geophysical loadings contained in the GPS observations is evaluated in this phase. Phase 3 concentrated on the tidal analysis of the harmonic and the tidal spectral to estimate the tidal parameters of amplitude and phase of the tidal constituents and to examine the characteristics of the geophysical loadings of the earth body tide, ocean tide loading and earth tide from the GPS observations. Lastly, phase 4 visualised the geophysical loadings response over the Malaysian region during the year 2013, during the apogee and perigee phenomenon and during the monsoon seasons. The research framework of this study is illustrated in Figure 1.5.

1.6.1 Phase 1: Literature Review and Planning

The literature review is concentrated on a few topics that are related to understanding the fundamentals of tides including the tides generating potential, the techniques of tidal analysis and the mechanism of the tides. The tidal effect of the geophysical loadings consisting of the earth body tide, ocean tide loading, atmospheric loadings and pole tides along with the sensor used to estimate this kind of geophysical loadings are also discussed in the literature review. The design of the planning phase involved the data acquisition and the processing strategy used in this study. There are three types of data acquired (1) the GPS observations along the year 2013 with the sampling rate of 30 seconds (2) the data predictions from the earth body tide model, IERS 2003 and (3) the data predictions from the ocean tide loading model, NAO.99b. In this study, the open source GPS/GNSS processing software known as Real-Time Kinematic Library (RTKLIB) is utilised for kinematic precise point positioning data processing. The programming language of MATLAB is also utilised to run the

solid.exe program to generate the IERS2003 model and the command prompt to run the GOTIC2 (Global Oceanic Tidal Correction) program to generate the NAO.99b model. Further details of the GPS processing method are discussed in Section 3.2.

1.6.2 Phase 2: The Correspondence of the Geophysical Loadings with the Theoretical Models

Phase 2 involved the estimation of the geophysical loadings that consist of the earth body tide, ocean tide loading and earth tide based on the GPS observations. This output undergoes data cleaning to remove noise as well as fill the gap contained in the time series for requirement of the tidal analysis purposes in phase 3. The outcome from the GPS is validated with the prediction from the theoretical models IERS2003 and NAO.99b to evaluate the agreement of correlation. Then, the presence of the earth body tide, ocean tide loading and earth tide is evaluated using the general least squares approach as discussed in Section 3.5 to discover the significance of the geophysical loading contribution to the GPS time series.

1.6.3 Phase 3: The Tidal Analysis

In this phase, the tidal assessment is performed by using the tidal harmonic analysis and tidal spectral analysis approaches to determine the amplitude and phase of the tidal constituents and to examine the characteristics of the earth body tide, ocean tide loading and earth tide. The computation of the tidal harmonic analysis and the tidal spectral analysis is elaborated in Section 2.2.2 and Section 2.2.4, respectively.

1.6.4 Phase 4: The Visualisation of the Geophysical Loadings Response over the Malaysian Region

Phase 4 is focused on the visualisation of the geophysical loadings response over the Malaysian region. The hourly snapshots of the geophysical loadings response are visualised using GMT 5.3.1 with surface interpolation. This spatio-temporal map is generated in several conditions, (1) the geophysical loadings variations along the year of 2013, (2) the geophysical loadings variations during the apogee and perigee phenomenon and (3) the geophysical loadings variations during the monsoon seasons. The conclusion of the study is based on the findings related to the aim and objectives achieved and the recommendation is provided to improve this study in the future.

1.7 Structure of the Thesis

This dissertation contains six chapters and these chapters are constructed as follows:

Chapter 1 Introduction

This chapter provided a background of the study on the implications of geohazard activities such as geophysical loadings in Malaysia towards the realization of the coordinate system in the geodesy field. The problem statement, aim and objectives of the study, the scope of the study and the significance of the study are also outlined in this chapter.

Chapter 2 Literature review

This chapter describes the basic theory of geophysical loadings and tides including tide generating potential and tidal analysis. The implementing of existing GPS CORS to support the understanding of earth tidal variations that consist of the earth body tide and ocean tide loading in the Malaysia region are discussed as well.

Chapter 3 Research methodology

This chapter discussed the GPS processing method and analysis technique used to achieve the objectives of the study. The estimation of the geophysical loadings from the GPS observations and the applicability of the prediction from the theoretical models, IERS2003 and NAO.99b is also elucidated in this chapter. Moreover, the details of the linear regression approaches for the data validation and the method of general least squares to estimate the presence of the geophysical loadings contained in the GPS observations is discussed.

Chapter 4 The correlation of GPS observations with the predictions of theoretical models

This chapter presents the results of the correlation of the earth body tide, ocean tide loading and earth tide from the GPS observations with the prediction from the theoretical models. The presence of geophysical loadings including earth tide, earth body tide and ocean tide loading in GPS observations is clarified in this chapter.

Chapter 5 The characteristics of earth body tide, ocean tide loading and earth tide observed by GPS

This chapter is the continuation from Chapter 4 which involves the tidal harmonic and tidal spectral analysis to determine the tidal parameters and the characteristic of geophysical loadings in GPS observations. The spatio-temporal variations of Earth tide displacements are generated in this chapter.

Chapter 6 Conclusions and recommendations

Finally, this chapter presents the conclusion of this study and the recommendations for further improvement in the future related study.

REFERENCES

- Abidin, H. Z. (2001). *Geodesi Satelit*. Edition 1. Jakarta: PT Pradnya Paramita.
- Abidin, H. Z. (2007). *Penentuan Posisi dengan GPS dan Aplikasinya*. Edition 3. Jakarta: PT Pradnya Paramita.
- Agnew, D. C. (1986). Strainmeters and tiltmeters. *Reviews of Geophysics*. 24 (3), 579-624.
- Agnew, D. C. (2009). *Earth Tides*. G. Schubert (Ed.) *Geodesy: Treatise on Geophysics*. (163-195). Radarweg 29, 1043 NX Amsterdam, the Nertherlands: Elsevier B. V.
- Ainee, A. (2016). *Derivation of Tidal Constituents from Satellite Altimetry Data for Coastal Vulnerability Assessment in Malaysia*. Degree of Master of Science (Geomatic Engineering). Faculty Geoinformation and Real Estate, Universiti Teknologi Malaysia, Malaysia.
- Allinson, C., Clarke, P., Edwards, S., King, M., Baker, T., and Cruddace, P. (2004). Stability of direct GPS estimates of ocean tide loading. *Geophysical research letters*. 31 (L15603), 1-4.
- BasicAstronomy. (2017). Apogee and Perigee of Moon in 2013. Retrieved from <http://www.basicastro.com/apogee-perigee-2013.html>
- Behrend, D. (2017). VLBI Network Stations. Retrieved from <https://ivscc.gsfc.nasa.gov/stations/ns-map.html>
- Berg, I. (2017). Tidal Cycles. Retrieved from http://beltoforion.de/article.php?a=tides_explained&p=tidal_cycles
- Bos, M. S., Penna, N. T., Baker, T. F., and Clarke, P. J. (2015). Ocean tide loading displacements in western Europe: 2. GPS-observed anelastic dispersion in the asthenosphere. *Journal of Geophysical Research: Solid Earth*. 120 (9), 6540-6557.
- Cai, C. (2009). *Precise point positioning using dual-frequency GPS and GLONASS measurements*. Degree of Master Science. Department of Geomatics Engineering, University of Calgary, Alberta.

- Dickey, J. O. (1995). *Earth Rotation*. T. J. Ahrens (Ed.) *Global earth physics: a handbook of physical constants*. (356-368). Washington, D.C: American Geophysical Union.
- Department of Survey and Mapping Malaysia (DSMM). (2012). Status of Surveying and Mapping in Malaysia. *Nineteenth United Nations Regional Cartographic Conference for Asia and the Pacific*. 29 October – 1 November 2012. Bangkok, 1-12.
- Dunncliff, J. (1993). *Geotechnical instrumentation for monitoring field performance*. Canada: John Wiley & Sons.
- El-Rabbany, A. (2002). *Introduction to GPS: The Global Positioning System*. Boston, London: Artech House.
- Elgazooli, B. A. G., and Ibrahim, A. M. (2012). Multiple gross errors detection in surveying measurements using statistical quality control. *Journal of Science and Technology*. Vol. 13 36-47.
- Farrell, W. E. (1972). Deformation of the Earth by surface loads. *Reviews of Geophysics*. 10 (3), 761-797.
- Ghilani, C. D., and Wolf, P. R. (2006). *Adjustment Computations Spatial Data Analysis*. 4th Edition. Inc., Hoboken, New Jersey: John Willey & Sons.
- Haas, R., Schuh, H., and Wünsch, J. (1996). Determination of tidal parameters from VLBI data. *11th Working Meeting on European VLBI for Geodesy and Astrometry*. Onsala, 162-171.
- Hall, R., van Hattum, M. W., and Spakman, W. (2008). Impact of India–Asia collision on SE Asia: the record in Borneo. *Tectonophysics*. 451 (1-4), 366-389.
- Héroux, P., and Kouba, J. (2001). GPS precise point positioning using IGS orbit products. *Physics and Chemistry of the Earth, Part A: Solid Earth and Geodesy*. 26 (6), 573-578.
- Hofmann-Wellenhof, B., Lichtenegger, H., and Wasle, E. (2007). *GNSS–Global Navigation Satellite Systems: GPS, GLONASS, Galileo, and more*. Austria: Springer Science & Business Media.
- International Hydrographic Organization (IHO). Harmonic Constituents with Nodal Corrections. Edition 1. Retrieved from https://www.iho.int/mtg_docs/com_wg/IHOTC/IHOTC8/Product_Spec_for_Exchange_of_HCs.pdf

- Ito, T., Okubo, M., and Sagiya, T. (2009). High resolution mapping of Earth tide response based on GPS data in Japan. *Journal of geodynamics*. 48 (3-5), 253-259.
- Jackson, S. L. (2009). *Research Methods and Statistics: A Critical Thinking Approach*. 3rd Edition. USA: Wadsworth Cengage Learning.
- Jamil, H., Mohamed, A., and Chang, D. (2010). The Malaysia real-time kinematic GNSS network (MyRTKnet) in 2010 and beyond. *FIG Congress 2010*. 11-16 April 2010. Sydney, Australia, 1-15.
- Katznelson, Y. (2004). *An introduction to harmonic analysis*. 3rd Edition. United Kingdom: Cambridge University Press.
- King, M., Colemar, R., and Nguyen, L. N. (2003). Spurious periodic horizontal signals in sub-daily GPS position estimates. *Journal of Geodesy*. 77 (1-2), 15-21.
- King, M. A., Penna, N. T., Clarke, P. J., and King, E. C. (2005). Validation of ocean tide models around Antarctica using onshore GPS and gravity data. *Journal of Geophysical Research: Solid Earth*. 110 (B08401).
- Longman, I. M. (1963). A Green's function for determining the deformation of the Earth under surface mass loads: 2. Computations and numerical results. *Journal of Geophysical Research*. 68 (2), 485-496.
- Marple, S. L. (1987). *Digital Spectral Analysis With Applications*. New Jersey: Prentice-Hall Englewood Cliffs.
- Martens, H. R., Simons, M., Owen, S., and Rivera, L. (2016). Observations of ocean tidal load response in South America from subdaily GPS positions. *Geophysical Journal International*. 205 (3), 1637-1664.
- MathBits. (2017). Correlation Coefficient. Retrieved from <https://mathbits.com/MathBits/TISection/Statistics2/correlation.htm>
- Matsumoto, K., Sato, T., Takanezawa, T., and Ooe, M. (2001). GOTIC2: A program for computation of oceanic tidal loading effect. *Journal of the Geodetic Society of Japan*. 47 (1), 243-248.
- Matsumoto, K., Takanezawa, T., and Ooe, M. (2000). Ocean tide models developed by assimilating TOPEX/POSEIDON altimeter data into hydrodynamical model: a global model and a regional model around Japan. *Journal of oceanography*. 56 (5), 567-581.

- McCarthy, D. D. (1996). *IERS Conventions (1996) (IERS Technical Note ; No. 21)*. Retrieved from International Earth Rotation And Reference Systems Service (IERS) Observatoire de Paris: www.iers.org
- McCarthy, D. D., and Petit, G. (2004). *IERS Conventions (2003) (IERS Technical Note ; No. 32)*. Retrieved from International Earth Rotation And Reference Systems Service (IERS) Germany: www.iers.org
- Meurers, B. (2001). Superconducting gravimetry in geophysical research today. *Journal of the Geodetic Society of Japan*. 47 (1), 300-307.
- Milbert, D. (2017). Solid Earth Tide. Retrieved from <http://geodesyworld.github.io/SOFTS/solid.htm>
- Neumeier, J. (2010). *Superconducting gravimetry*. G. Xu (Ed.) *Sciences of Geodesy- I Advances and Future Directions*. (339-413). Germany: Springer.
- Pagiatakis, S. D. (1988). *Ocean tide loading on a self-gravitating, compressible, layered, anisotropic, viscoelastic and rotating earth with solid inner core and fluid outer core*. Degree of Doctor of Philosophy. Department of Surveying Engineering, University of New Brunswick, Fredericton, N. B. Canada.
- Pahlevi, A. M. (2016). *Investigation of Geophysical Effects on GPS Positioning*. Degree of Master of Engineering. Faculty of Earth Science and Technology, Institute Technology of Bandung, Indonesia.
- Pahlevi, A. M., Prijatna, K., Meilano, I., and Sofian, I. (2017). Investigation of the solid earth tide based on GPS observation and superconducting gravimeter data. *GEOMATIKA*. 22 (1), 29-36.
- Penna, N. T., Clarke, P. J., Bos, M. S., and Baker, T. F. (2015). Ocean tide loading displacements in western Europe: 1. Validation of kinematic GPS estimates. *Journal of Geophysical Research: Solid Earth*. 120 (9), 6523-6539.
- Petrov, L., and Boy, J. (2004). Study of the atmospheric pressure loading signal in VLBI observations. *Journal Geophysical Research*. 109 (B03405).
- Pugh, D., and Woodworth, P. (2014). *Sea-level science: understanding tides, surges, tsunamis and mean sea-level changes*. Cambridge University Press.
- Putri, N. S. E. (2014). *Land-Sea Mask Modelling for Atmospheric Pressure Loading Determination*. Degree of Master of Engineering. Faculty of Earth Science and Technology, Institute of Technology of Bandung, Indonesia.
- Rappel, W., and Schuh, H. (1986). The influence of atmospheric loading on VLBI-experiments. *Journal of Geophysics-Zeitschrift fuer Geophysik*. 59 164-170.

- Raziq, N., and Collier, P. (2006). *High precision GPS deformation monitoring using single receiver carrier phase data*. F. Sansò & A. J. Gil (Ed.) *Geodetic Deformation Monitoring: From Geophysical to Engineering Roles*. (95-102). Berlin Heidelberg New York: Springer.
- Richter, B. (1998). A New Generation of Superconducting Gravimeters. *Proc. 13th Symp. Earth Tides*. 22-25 July, 1997. Brussels, 545-555.
- Roberts, D. (2017). Correlation Coefficients. Retrieved from <https://mathbitsnotebook.com/Algebra1/StatisticsReg/ST2CorrelationCoefficients.html>
- Saito, M. (1967). Excitation of free oscillations and surface waves by a point source in a vertically heterogeneous earth. *Journal of Geophysical Research*. 72 (14), 3689-3699.
- Scherneck, H. G. (1991). A parametrized solid earth tide model and ocean tide loading effects for global geodetic baseline measurements. *Geophysical Journal International*. 106 (3), 677-694.
- Schuh, H., and Behrend, D. (2012). VLBI: A fascinating technique for geodesy and astrometry. *Journal of geodynamics*. 61, 68-80.
- Schureman, P. (1971). *Manual of harmonic analysis and prediction of tides*. United States: U.S. Department of Commerce Coast and Geodetic Survey.
- Smith, S. W. (1999). *The scientist and engineer's guide to digital signal processing*. Edition 2. California: California Technical Publishing.
- Subirana, J. S., Zornoza, J. M. J., and Hernández-Pajares, M. (2013). *GNSS data processing, Vol. I: Fundamentals and algorithms*. Netherlands: ESA Communications.
- Thomas, I. D., King, M. A., and Clarke, P. J. (2007). A comparison of GPS, VLBI and model estimates of ocean tide loading displacements. *Journal of Geodesy*. 81 (5), 359-368.
- Thomson, R. E., and Emery, W. J. (2014). *Data analysis methods in physical oceanography*. Edition 3. Amsterdam, The Netherlands: Elsevier.
- Towhiduzzaman, M., Asaduzzaman, A. Z. M., and Ullah, M. A. (2017). Calculation of the Speeds of Some Tidal Harmonic Constituents. *International Journal of Advance Research and Innovative Ideas in Education, Online ISSN-2395-4396*. Vol. 3 (Issue-1), 598-604.

- Tuttas, S. (2011). *Joint gravimetric and geometric survey of geophysical signals- Feasibility study for the TERENO alpine and prealpine Ammer observatory*. Degree of Master of Satellitengeodäsie. Institut für Astronomische und Physikalische Geodäsie, Technische Universität München.
- Vella, J. P. (2000). *The Development of Tide Models for the Exclusive Economic Zone (EEZ) of Malaysia Using Satellite Altimetry*. Degree of Master of Science (Geoinformatics). Faculty of Geoinformation Science and Engineering, Universiti Teknologi Malaysia, Malaysia.
- Vey, S., Calais, E., Llubes, M., Florsch, N., Woppelmann, G., Hinderer, J., Amalvict, M., Lalancette, M. F., Simon, B., Duquenne, F., and Haase, J. S. (2002). GPS measurements of ocean loading and its impact on zenith tropospheric delay estimates: a case study in Brittany, France. *Journal of Geodesy*. 76 (8), 419-427.
- Viswanathan, M. (2013). *Simulation of digital communication systems using Matlab*. Edition 2. Amazon: Mathuranathan Viswanathan.
- Wahr, J. M. (1985). Deformation induced by polar motion. *Journal of Geophysical Research: Solid Earth*. 90 (B11), 9363-9368.
- Warburton, R. J., and Brinton, E. W. (1995). *Recent developments in GWR instruments' superconducting gravimeters*. Paper presented at the Proc. 2nd Workshop on Non-tidal Gravity Changes: Intercomparison Between Absolute and Superconducting Gravimeters.
- Wijaya, D. D. (2012a). *Pengantar Fourier Series*. Unpublished note, Kelompok Keilmuan Geodesi, Institut Teknologi Bandung, Indonesia.
- Wijaya, D. D. (2012b). *Pengantar Fourier Transform*. Unpublished note, Kelompok Keilmuan Geodesi, Institut Teknologi Bandung, Indonesia.
- Wijaya, D. D. (2017). *Discussion on estimation of the geophysical loadings*. Unpublished note, Kelompok Keilmuan Geodesi, Institut Teknologi Bandung, Indonesia.
- Yan, X., and Su, X. (2009). *Linear regression analysis: theory and computing*. Singapore: World Scientific Publishing Co. Pte. Ltd.
- Yong, C. Z. (2013). *Developing Continuous Displacement Detection System for Geohazards Monitoring*. Degree of Master of Science. Faculty of Geoinformation and Real Estate, Universiti Teknologi Malaysia, Malaysia.

- Yuan, L., Chao, B. F., Ding, X., and Zhong, P. (2013). The tidal displacement field at Earth's surface determined using global GPS observations. *Journal of Geophysical Research: Solid Earth*. 118 (5), 2618-2632.
- Zheng, Y. (2007). *Generation of network-based differential corrections for regional GNSS services*. Degree of Doctor of Philosophy. Faculty of the Built Environment and Engineering, Queensland University of Technology, Australia.